remote sensing

MDPI

Article

Mapping Coastal Marine Habitats Using UAV and Multispectral Satellite Imagery in the NEOM Region, Northern Red Sea

Emma Sullivan [1,2,†], Nikolaos Papagiannopoulos [3,†], Daniel Clewley [2,4], Steve Groom [1,2], Dionysios E. Raitsos [5] and Ibrahim Hoteit [3,*]

[1] Earth Observation Science and Applications (EOSA), Plymouth Marine Laboratory (PML), Plymouth PL1 3DH, UK; emsu@pml.ac.uk (E.S.); sbg@pml.ac.uk (S.G.)
[2] NERC Earth Observation Data Analysis and AI Service (NEODAAS), National Centre for Earth Observation, Plymouth PL1 3DH, UK; dac@pml.ac.uk
[3] Earth Science and Engineering (ErSE), King Abdullah University of Science and Technology (KAUST), Thuwal 23955, Saudi Arabia; nikolaos.papagiannopoulos@kaust.edu.sa
[4] Digital Innovation and Marine Autonomy (DIMA), Plymouth Marine Laboratory (PML), Plymouth PL1 3DH, UK
[5] Department of Biology, National and Kapodistrian University of Athens, 15772 Athens, Greece; draitsos@biol.uoa.gr
* Correspondence: ibrahim.hoteit@kaust.edu.sa
† These authors contributed equally to this work.

Abstract: Effective management to conserve marine environments requires up-to-date information on the location, distribution, and extent of major benthic habitats. Remote sensing is a key tool for such assessments, enabling consistent, repeated measurements over large areas. There is particular interest in using freely available satellite images such as from the Copernicus Sentinel-2 series for accessible repeat assessments. In this study, an area of 438 km^2 of the northern Red Sea coastline, adjacent to the NEOM development was mapped using Sentinel-2 imagery. A hierarchical Random Forest classification method was used, where the initial level classified pixels into a geomorphological class, followed by a second level of benthic cover classification. Uncrewed Aerial Vehicle (UAV) surveys were carried out in 12 locations in the NEOM area to collect field data on benthic cover for training and validation. The overall accuracy of the geomorphic and benthic classifications was 84.15% and 72.97%, respectively. Approximately 12% (26.26 km^2) of the shallow Red Sea study area was classified as coral or dense algae and 16% (36.12 km^2) was classified as rubble. These reef environments offer crucial ecosystem services and are believed to be internationally important as a global warming refugium. Seagrass meadows, covering an estimated 29.17 km^2 of the study area, play a regionally significant role in carbon sequestration and are estimated to store 200 tonnes of carbon annually, emphasising the importance of their conservation for meeting the environmental goals of the NEOM megaproject. This is the first map of this region generated using Sentinel-2 data and demonstrates the feasibility of using an open source and reproducible methodology for monitoring coastal habitats in the region. The use of training data derived from UAV imagery provides a low-cost and time-efficient alternative to traditional methods of boat or snorkel surveys for covering large areas in remote sites.

Keywords: Red Sea; NEOM; benthic habitat; classification; Sentinel-2; coral reef; seagrass meadows; mapping

check for updates

Academic Editor: Jorge Vazquez

Received: 11 October 2024
Revised: 14 January 2025
Accepted: 23 January 2025
Published: 30 January 2025

Citation: Sullivan, E.; Papagiannopoulos, N.; Clewley, D.; Groom, S.; Raitsos, D.E.; Hoteit, I. Mapping Coastal Marine Habitats Using UAV and Multispectral Satellite Imagery in the NEOM Region, Northern Red Sea. *Remote Sens.* **2025**, *17*, 485. https://doi.org/10.3390/rs17030485

Copyright: © 2025 by the authors. Licensee MDPI, Basel, Switzerland. This article is an open access article distributed under the terms and conditions of the Creative Commons Attribution (CC BY) license (https://creativecommons.org/licenses/by/4.0/).

1. Introduction

The Red Sea is a narrow body of water located between the African and Asian continental shelves with an area of approximately 438,000 km^2 and length of over 2000 km [1]. It connects with the Indian Ocean through the Gulf of Aden and the Mediterranean Sea via the Suez Canal, making the Red Sea one of the most important trade routes globally, particularly for petroleum products [2]. It is one of the warmest and most saline water bodies in the world and hosts diverse marine ecosystems, including near-continuous tracts of mainland- and island-fringing coral reefs along its coast [3]. These marine ecosystems have high taxonomic diversity and high levels of endemism, and as a result, the Red Sea is considered a biodiversity hotspot [3–5]. The northern Red Sea (NRS) in particular has been identified as a conservation priority because of its habitat complexity, endemic species, and heat-tolerant corals with unique symbiont genotypes, which could serve as a global warming refugium [3,5–8]. Beyond their biological importance [9], the complex reef systems and lagoons along Saudi Arabia's NRS coastline also have considerable social and economic value [10–13].

However, these coastal ecosystems are expected to encounter increasing pressures in upcoming decades [14]. Globally, marine ecosystems are under threat from a range of direct and indirect anthropogenic stressors, including climate change, overfishing, pollution, and coastal development. While coral reefs in the NRS have historically experienced relatively low levels of direct human disturbance [15], this area is one of the fastest warming tropical marine ecosystems worldwide [16–19] and has been subject to a significant increase in marine heatwaves during the past decades [20]. These heatwave events can cause even heat-tolerant corals to bleach if their bleaching threshold is exceeded [21,22]. The combination of increasing water temperatures and frequency of marine heatwave events may impact organisms' future resilience and persistence in the NRS. Compounding these environmental pressures, this area is also witnessing one of the most ambitious development plans in history [23]. NEOM is a USD 500 bn megaproject to develop a new city in Tabuk Province in the northwestern region of Saudi Arabia. It is part of the Saudi 2030 vision, which plans to expand the country's non-oil economy [24]. Some of the planned projects will extend directly into marine ecosystems, and the coastline is likely to be a major attraction for visitors in the future. Despite these challenges, the NEOM development project has made a commitment to preserve 95% of the land and sea within designated protected areas and aims to develop world-class approaches to conservation and ecosystem regeneration [25].

Effective management to protect marine environments requires up-to-date information on the location, distribution, and extent of major benthic habitats [26,27]. Satellite remote sensing is an effective tool for such assessment, as it enables consistent, repeated measurements over large areas [28]. While remote sensing cannot provide the accuracy and level of detail that field surveys deliver, it can be used to assess large-scale spatial patterns in habitat cover [29]. Previous mapping exercises conducted in the region are either relatively old, are not publicly accessible, focus on smaller areas, lack localised accuracy assessment, or are not derived from automated methods. These factors collectively present challenges in terms of repeatability and relevance for regional stakeholders. The first major mapping effort in this region was undertaken by the Japan International Cooperation Agency (JICA) and the Saudi National Commission for Wildlife Conservation and Development (NCWCD), who produced habitat maps for the NRS coast of Saudi Arabia using aerial photography [30]. Images and video collected during 1998–1999 were hand-interpreted with knowledge from ground surveys used to revise and verify classes. This provided an inventory for the whole area but is now over two decades old and is resource-intensive to reproduce. More recently, a large-scale mapping effort classified five individual sites along the Saudi Arabian Red Sea coast using a combination of Landsat-7 ETM+, QuickBird satellite imagery, and AISA Eagle

airborne hyperspectral images, as well as in situ observations [1]. The study produced a high-resolution map with a detailed benthic classification scheme, but it only covered a small part of the NEOM region (Ras Al-Qasabah) and is not easily replicable due to the data sources used. There are also several global mapping and modelling projects, such as the Allen Coral Atlas [31], the Global Distribution of Coral Reefs [32], the Global Distribution of Seagrasses [33], the modelled global distribution of the seagrass biome [34] and the global reef probability map [35], that cover the Red Sea. However, due to their nature as global products, they have limited local validation and accuracy assessment. While the Allen Coral Atlas offers a recent classification at a high spatial resolution of 5 m, as a global-scale product, it is likely performance will vary between locations at a site scale [31]. It is also acquired from commercial imagery, which may limit the temporal resolution available for managers. Considering these limitations, within the NEOM region, there is a need for a localised and repeatable mapping approach for effective resource management and biodiversity preservation.

The creation of benthic thematic maps typically requires continuous geospatial datasets that serve as predictor variables, in combination with 'ground-truthing' observations, which are used to train and validate the classification model [36,37]. For the last decade, optical technologies have been the most utilised approach for obtaining these continuous geospatial datasets [36], with studies ranging from local-scale studies using high-resolution drone imagery [38–40] to regional and global efforts mapping and monitoring entire reef systems using freely-available moderate-resolution satellite imagery and commercial imagery such as PlanetScope or WorldView-3 [31,41]. While recent studies have demonstrated that high-resolution imagery such as WorldView can have superior performance in terms of accuracy in benthic mapping [42], its use in regional-scale studies is often constrained by cost, temporal resolution, and coverage, making it more suited to smaller sites where maximising accuracy and identifying boundaries are the priority [42,43]. On the other hand, medium-resolution, freely available optical imagery has been extensively used for larger-scale mapping projects, enabling significant progress in mapping vast reef areas [44], and it is suitable for assessing general patterns of benthic cover. Until 2016, these data were primarily from the Landsat series of sensors (at 30 m resolution), which have been providing imagery since 1984. However, in 2015, the first of the Sentinel-2 series of satellites was launched. This constellation of two satellites provides optical data over coastal waters with a maximum 10 m spatial resolution, which is a significant improvement over earlier freely accessible optical satellite datasets [45]. Recent studies have demonstrated the effectiveness of using Sentinel-2 imagery for mapping tropical reefs and seagrass habitats [26,46,47]. Therefore, Sentinel-2 offers a promising approach for the accurate, large-scale, and cost-effective mapping of the benthic habitats of the NRS.

One of the key challenges of this study area, as with many other remote reefs, is the collection of ground-truthing points given the scale and the accessibility of the site. The most common form of ground-truthing for benthic mapping efforts is underwater imagery or surveys [36]. However, at the time this study was conceived, boat, snorkel, or diver surveys were challenging due to the effort needed to cover large areas, the remote desert location, and restrictions in place due to the NEOM development project. In previous studies where these data are unavailable or limited, researchers have used other sources of data for training and validation, including high-quality existing maps [46], and the interpretation of satellite imagery [48] or high-resolution airborne data and drone data [26,49,50] to ground-truth lower-resolution maps. UAV surveys offer a promising method for generating training and validation data in regions like the NRS, as they allow surveyors to rapidly cover large, potentially inaccessible areas and capture high-resolution imagery. As UAV technology becomes more affordable and widely available, these surveys may provide an

accessible means to assess benthic cover quickly with minimal disturbance. In this study, we will utilise UAV surveys as a source of training and validation data and discuss the associated benefits and challenges of this method.

The primary objective of this work is to create maps of geomorphic and benthic habitats for the entire NEOM region and establish a reproducible and open-source mapping approach suitable for monitoring and planning. We explore the feasibility of using Sentinel-2 imagery in combination with high-resolution UAV imagery for the validation of these classification maps as a cost-effective and non-intrusive methodology. Using this method, we create maps of geomorphic and benthic habitats for the entire NEOM region at a 10 m spatial resolution and assess their accuracy. Accurate and up-to-date maps of this area can benefit conservation efforts and sustainable development planning. Additionally, this work will serve as a foundation for further studies on biodiversity hotspots and the continuous operational monitoring of marine habitats in the NEOM region and the Red Sea.

2. Materials and Methods

2.1. Study Area: NEOM

This study covered the shallow waters of the Saudi Arabian NRS from 27.63°N to 28.60°N (Figure 1). This stretch of coastline is complex, with many small bays and islands. Much of the coastline is characterised by fringing reefs, but several areas display diverse reef morphologies, including patch reefs, complex reticulate reefs, and offshore atolls [3,51]. Other shallow marine habitats reported in this area include seagrass beds, algal mats, subtidal sand flats, and coastal sand or mud flats [1,52]. The climate is arid with non-perennial rivers, and offshore sea surface temperatures typically range between 23 °C (winter) and 29 °C (summer), and salinities are typically around 40.5 ppt [1,9,53].

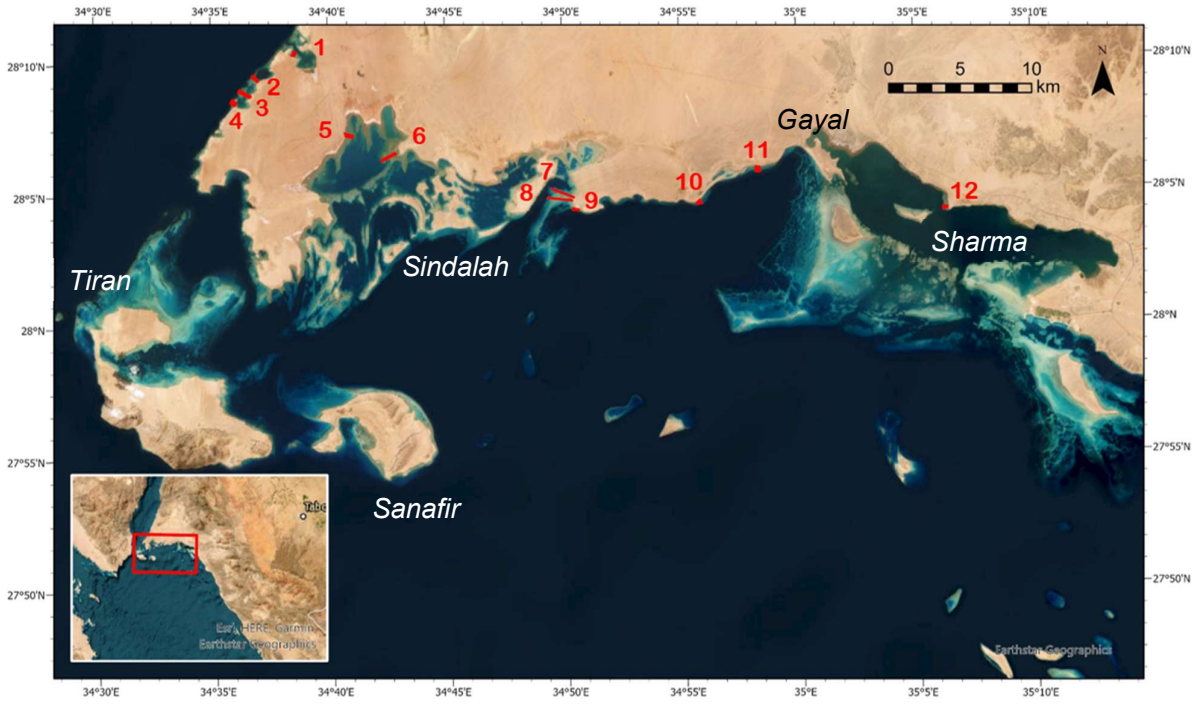


Figure 1. Map of Uncrewed Aerial Vehicle sampling stations in NEOM. Sites 2, 4, 6, 7, 9, and 11 were used for training, while sites 1, 3, 5, 8, 10, and 12 were used for validation. Satellite image ESRI basemap is from Earthstar Geographics.

2.2. UAV Field Data Collection

UAV surveys were undertaken to collect data on benthic cover for model training and validation purposes. UAV surveys were chosen because they enabled the coverage of

large areas and because organising boat, snorkel, or diver surveys was not possible due to the remote location and restrictions in place due to the NEOM development project. UAV surveys were carried out at 12 locations along the NEOM coast covering a diverse range of benthic habitats (Figure 1) during November 2021. A DJI Matrice 300 RTK was used along with a mounted DJI Zenmuse P1 42 MP RGB camera. The UAV was equipped with a Real-Time Kinetic system, which included a Global Navigation Satellite System rover that provided a spatial accuracy of ~2 cm. The surveys were conducted at an altitude of 80 m and captured RGB images with a resolution of ~2 cm every 13 m, with 75% side and 80% frontal overlap. Survey times with a high sun zenith angle and low wind speed were selected to reduce the impact of sun glint and waves. All the collected images were quality-assessed to ensure accurate geo-referencing and merged into orthomosaic images with ~3 cm resolution. Images without any reference points such as coral or large rocks (i.e., consisting only of deep waters) were not included in the process, as it was not feasible to overlap and accurately georeference them.

Training and validation points were generated using a stratified random sampling approach based on an initial geomorphic classification of the sites trained using points interpreted from a high-resolution Google basemap to obtain a random sample with representative coverage across the different environments found in this area. A 10 × 10 m grid was created to reflect the footprint of the Sentinel-2 composite pixels and overlaid over the UAV imagery. Each point was assigned a class based on the majority cover of the grid square. If there was uncertainty in the class due to water depth or clarity, or an equal cover of two classes, the point was marked as 'unclassified' and discarded from the training/validation dataset. The sample points were assigned a class manually using the QGIS Class Accuracy plugin. UAV image interpretation was split between two people, with the first site being interpreted together and one site assessed by both people, which enabled the calculation of an agreement score of 94%. Once completed, the dataset was split by site, with half of the survey sites used for training and the other half for validation. The decision to split the training and validation data by site, rather than randomly, was taken to try to more robustly assess the accuracy of applying the classifier in locations away from the training sites. Additional training points were added from visual interpretation of the UAV imagery in the training sites to balance the classes.

2.3. Sentinel-2 Imagery Pre-Processing

The adopted methodology for image pre-processing and the classification of benthic habitats is outlined in Figure 2. An annual median composite image of the study area was created using Sentinel-2 imagery from 2021. The area of interest covers four Sentinel-2 tiles (36RXR, 36RXS, 36RYR, 36RYS). The 20 m and 60 m bands were resampled to 10 m resolution, and the images were merged and atmospherically corrected using ACOLITE version 20220222.0, an atmospheric correction processor developed for aquatic applications, which has been shown to provide robust and consistent results for Sentinel-2 scenes over coastal waters [54–56]. In total, 590 scenes were processed. Land and clouds were masked using ACOLITE flags, while deep waters were masked using a band 3 (560 nm) surface reflectance threshold value of 0.033. Pixels with fewer than 12 observations in the year, primarily residual unmasked land, were excluded from the analysis. In some previous studies, applying water column correction has been shown to improve the accuracy of benthic habitat mapping by removing the confounding influence of variable water depth (e.g., [57,58]). In this work, the 'depth-invariant bottom index' approach [59] was used to calculate three depth-invariant index (DII) bands from the blue–green, blue–red, and green–red band pairs.

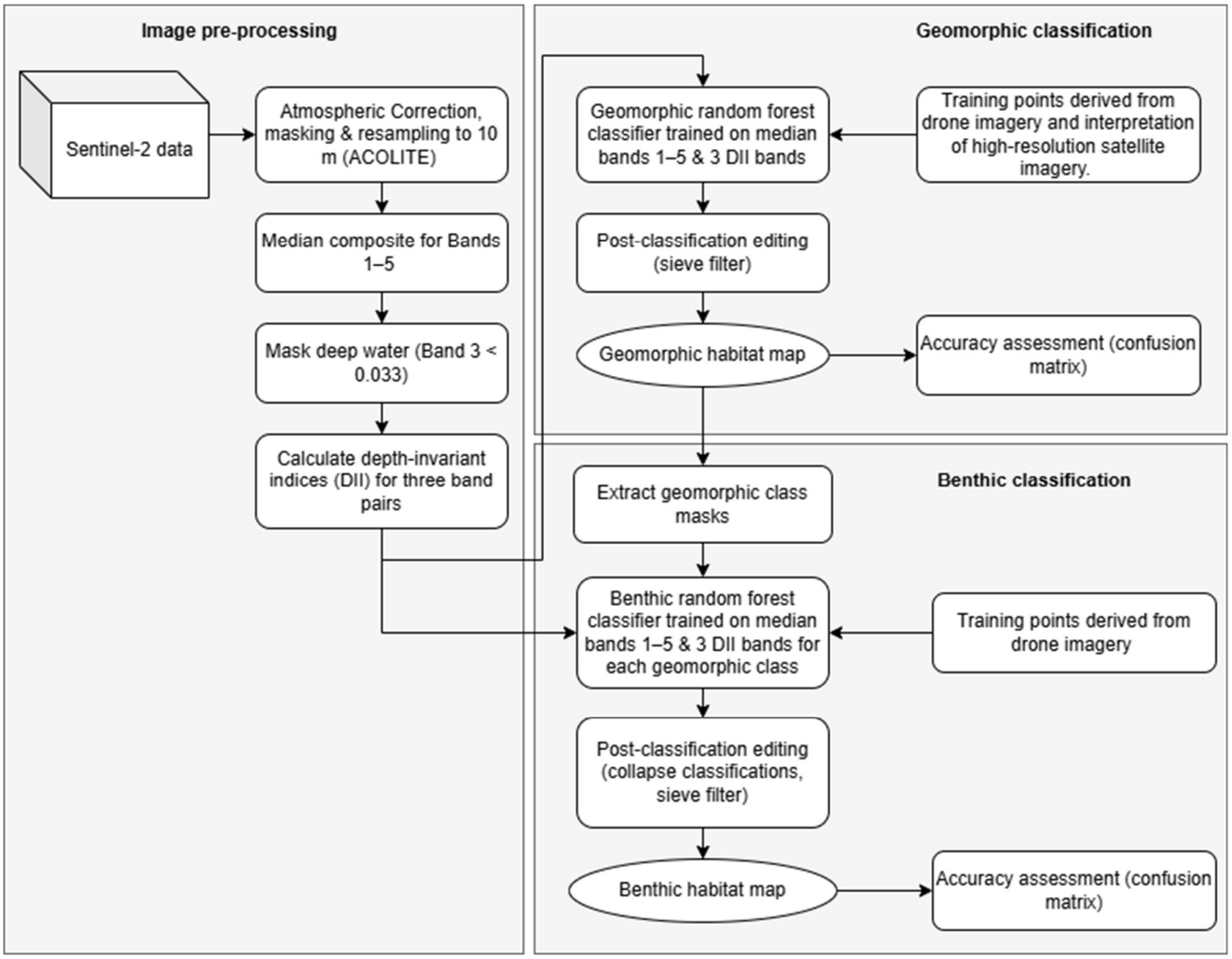


Figure 2. Flowchart diagram summarising the methodology adopted for the supervised classification of Red Sea benthic habitats in the NEOM area.

2.4. Classification

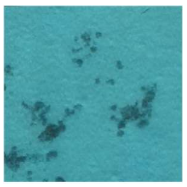
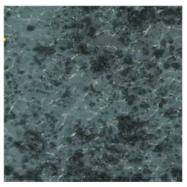
A hierarchical classification approach with two levels was adopted for classifying marine habitats in the study area. The first level is a geomorphological classification, separating distinct reef zones caused by physical parameters such as the depth, slope, and exposure of the reef [60,61]. Geomorphological classes can provide useful ecological information because specific communities are found in these different zones. The second level is a benthic cover classification, which contains classes based on the species composition of an area, which is of direct interest for conservation and monitoring but more challenging to interpret from medium-resolution imagery, as this can be highly heterogeneous over smaller spatial scales [60,61]. The geomorphic classification scheme for this work is based on the Reef Cover Classification from [60], with some amendments for the study area and the resolution of Sentinel-2 imagery. For example, sheltered walls, walls, reef slopes, and sheltered slopes are not included as separate classes due to the shallow maximum depth of observation and the spatial resolution of Sentinel-2 imagery. Furthermore, an additional class has been added for sand/mud flat areas, which are found in several bays in this region. A complete description of each class can be found in Tables 1 and 2.

Table 1. Descriptions of the six geomorphic classes selected for classifying shallow waters in the NEOM region. Each class represents a different underwater environment shaped by their geology and dominant processes.

Class	Description
Reef crest	The reef crest is the shallow zone that separates the reef flat and the reef slope. It is generally shallow with high wave energy absorbance [60]. In some locations, reef crests may be emergent. They are usually dominated by coralline algae in the breaker zone with live coral in deeper areas [60]. In the central-northern Red Sea, exposed coral crests are associated with species of *Acropora*, *Pocillopora*, *Stylophora*, *Merulinidae*, and *Favia* [1,3,62]. Live coral cover is typically high [1,62]. In this classification, the reef front or reef slope, the submerged, sloping area extending seaward from the reef crest towards the shelf break, is also included in this class.
Outer reef flat	The outer reef flat is at the seaward edge of the reef behind the reef crest and is a broad and shallow platform with zonation caused by wave exposure [60]. It is typically shallower, flatter, and more exposed compared to the inner reef flat. The outer reef flat is often dominated by hard substrate, and benthos are often harder with more coral and coralline algae [60].
Inner reef flat	The inner reef flat is a flat or gently sloping platform behind the outer reef flat [60]. It is typically sediment-dominated, with lower exposure than the outer reef flat. There is generally less living coral compared to the outer reef flat, and internal zonation is less pronounced [60].
Shallow lagoon	A shallow lagoon is any sheltered shallow water area, which is sediment-dominated and enclosed or semi-enclosed by a reef. Shallow lagoon areas are often dominated by bare sediment, likely to be coarse sand and coralline rubble; live coral cover is typically low [1].
Deep water	Deep water covers any body of water where the bottom is beyond remote sensing depth detection limits and where water is too deep for a class to be interpreted from UAV imagery. This class may still contain deep coral and seagrass beds but should be investigated with alternative methods.
Sand and mud flats	Sand and mud flats are sand- or mud-dominated areas where sediment may be exposed at low tide. Substrate may be covered by filamentous or calcareous macroalgae or cyanobacteria [1,30].

The Random Forest machine learning classifier from scikit learn within the RSGISLib library was used for classification [63,64]. This algorithm is widely used in benthoscape mapping [36,65], and previous studies have shown it compares favourably to other algorithms [26,66,67]. Different supervised learning models, such as support vector machines and neural networks, were also evaluated in the initial stages of the project, but Random Forest returned results with a higher overall accuracy and was, therefore, chosen for this study. Sentinel-2 MSI reflectance bands 1 to 5 and three DII bands were used for both classification levels. The geomorphic classifier was trained with both training points from the UAV imagery training sites, and points were interpreted from a high-resolution Google basemap. The image was then segmented based on its geomorphic class, and for each zone, a benthic classifier was trained for the corresponding benthic classes (Table 2). Due to the scale and complexity of interpreting benthic cover, only points interpreted from the high-resolution UAV imagery were used to train the benthic classifier. The Jeffries–Matusita distances for both the benthic and geomorphic classes were calculated using the method described by Richards (2013) [68] from the Sentinel-2 reflectance bands.

Table 2. Descriptions for the six benthic habitat classes used for classifying shallow waters in the NEOM region. The locations indicate the geomorphic classes each benthic class is associated with. Example images are taken from the Uncrewed Aerial Vehicle survey areas.

Class	UAV Image	Description
Coral/algae dominated		Areas of hard underlying framework with coral or dense macroalgae patches. Includes areas of small or patch reefs. Location: reef crest, outer reef flat, inner reef flat, and shallow lagoon.
Seagrass		Areas of soft substrate with single or mixed seagrass species assemblages. Generally found in shallow sheltered areas, but dense monospecific assemblages also occur in deep sandy environments in the Red Sea [1]. Location: inner reef flat, sand and mud flats, and shallow lagoon.
Lagoon sand		Areas of soft substrate where bright sand dominates. Location: inner reef flat, sand and mud flats, and shallow lagoon.
Rubble		This class is broad and covers areas with a mix of rubble (loose fragments of broken reef material), sparse corals, and sand. Location: reef crest, outer reef flat, inner reef flat, and shallow lagoon.
Shallow sandflats and mudflats		Shallow sand- or mud-dominated areas. Substrates may be covered by filamentous or calcareous macroalgae or cyanobacteria [1,30]. Location: inner reef flat, sand and mud flats, and shallow lagoon.
Rock		Rock describes areas dominated by exposed areas of hard bare substratum, beach rock, or pavement. This is often associated with areas of high wave energy. Location: reef crest, outer reef flat, and inner reef flat.

2.5. Validation

The classification was validated using 944 points extracted from six UAV survey areas using the method described above in Section 2.2. The results of the validation are reported as an error matrix in terms of the proportion of the area, and this was used to derive the overall accuracy of the map (the proportion of the area classified correctly), user's accuracies (the proportion of the area classified as class *i* that is also class *i* in the reference data), and producer's accuracies (the proportion of the area that is reference class *j* and is also class *j* in the map), based on the method described by Olofsson et al., 2014 [69]. The area estimate of each class was adjusted based on the reference data to account for map biases and provide uncertainty estimates [69,70].

3. Results

3.1. Earth Observation Data Processing

The output from the earth observation data pre-processing was a composite Sentinel-2 image for 2021, with cloud and glint removed and with three additional bands derived from water column correction (Figure 3). Visual interpretation of the imagery highlights the varied nature of the Saudi Arabian coastline of the NRS, which includes rocky shores, small bays, and sandy and muddy beaches. The imagery also allows for the identification of various coral reef types, such as reticulated reef structures, fringing reefs, and patch reefs.

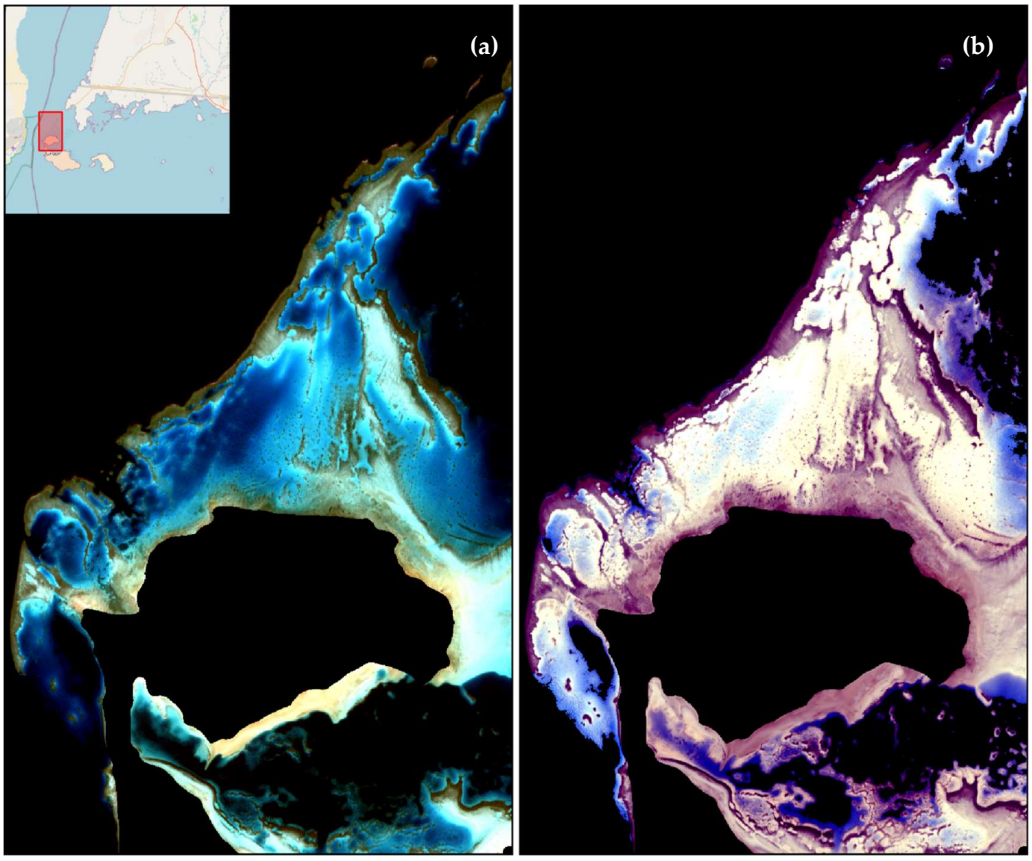


Figure 3. (**a**) True colour composite image of Tiran Island, northern Red Sea, after atmospheric correction and compositing scenes. (**b**) False colour image of the same area using depth invariant indices. The red channel of the image is the green–red DII, the green channel is the blue–red DII, and the blue channel is the green–blue DII. Land and deep water are masked in black.

3.2. Habitat Classification Scheme

The Jeffries–Matusita (JM) distances were examined to estimate the spectral separability of the classes. The JM distance ranges from 0 to 2, where 0 indicates identical classes and 2 indicates completely different classes [67]. Over half of the class pairs had a JM distance of $\geq$1.9, indicating good separability, while all class pairs had a JM distance of at least 1.3 (Table 3). The lowest separability values for the benthic classification were for rubble and coral (1.33) and rubble and seagrass (1.34), indicating that rubble in particular will be potentially challenging to accurately map. The lowest separability for the geomorphic classes was between the inner and outer reef flat (1.5).

Table 3. Jeffries–Matusita separability measured between the geomorphic and benthic classes in the NEOM region, northern Red Sea. Values can range between 0 and 2, with 0 being identical and 2 completely different. Asterisk indicates pairs with poor separability (<1.9).

Level 1: Geomorphic		
Class 1	**Class 2**	**Jeffries–Matusita Separability**
Inner reef flat	Outer reef flat	1.50 *
Crest	Inner reef flat	1.62 *
Crest	Outer reef flat	1.69 *
Inner reef flat	Sand and mud flats	1.79 *
Inner reef flat	Shallow lagoon	1.82 *
Water	Crest	1.86 *
Water	Shallow lagoon	1.91
Crest	Shallow lagoon	1.94
Crest	Sand and mud flats	1.97
Outer reef flat	Sand and mud flats	1.97
Water	Inner reef flat	1.98
Outer reef flat	Shallow lagoon	1.99
Sand and mud flats	Shallow lagoon	1.99
Water	Sand and mud flats	1.99
Water	Outer reef flat	2.00
Level 2: Benthic		
Class 1	**Class 2**	**Jeffries–Matusita Separability**
Coral/algae dominated	Rubble	1.33 *
Rubble	Seagrass	1.34 *
Seagrass	Lagoon sand	1.66 *
Rubble	Lagoon sand	1.66 *
Coral/algae dominated	Seagrass	1.70 *
Coral/algae dominated	Lagoon sand	1.81 *
Coral/algae dominated	Rock	1.88 *
Shallow sandflats and mudflats	Rubble	1.94
Shallow sandflats and mudflats	Seagrass	1.95
Rock	Rubble	1.98
Shallow sandflats and mudflats	Lagoon sand	1.99
Coral/algae dominated	Shallow sandflats and mudflats	2.00
Shallow sandflats and mudflats	Rock	2.00
Rock	Lagoon sand	2.00
Rock	Seagrass	2.00

3.3. Image Classification

In total, an area of 438 km^2 was mapped along 566 km of the northern Saudi Arabian coastline. Figures 4–7 show maps of selected sites in the study area. Sand and mudflats dominated the near-shore environments, with long stretches of fringing reef flats along the coast and around islands and a seaward reef crest dominated by coral or rubble. The error matrices expressed in terms of proportion of area are presented in Tables 4 and 5, and the accuracy statistics and predicted areas for all classes are presented in Table 6.

The geomorphic classification's (Figures 4 and 6) overall accuracy was 84.15% (Table 6). All geomorphic classes had producer's accuracies >70%, with the highest values observed for the deep water, reef crest, and inner reef flat classes (>77% Table 6). The outer reef flat class had the lowest producer's accuracy, with reference points most frequently misclassified as inner reef flats (Table 4 and Table S2). The classes with the highest user's accuracies were sand and mud flats, shallow lagoons, and deep water. The reef crest and outer reef flat classes had the lowest user's accuracies. Excluding deep water areas, the most abundant geomorphic class was the shallow lagoon class (103.6 km^2), followed by the

inner reef flat (56.1 km^2), the sand/mud flat (46.6 km^2), the outer reef flat (15.6 km^2), and the reef crest (13.9 km^2) classes.

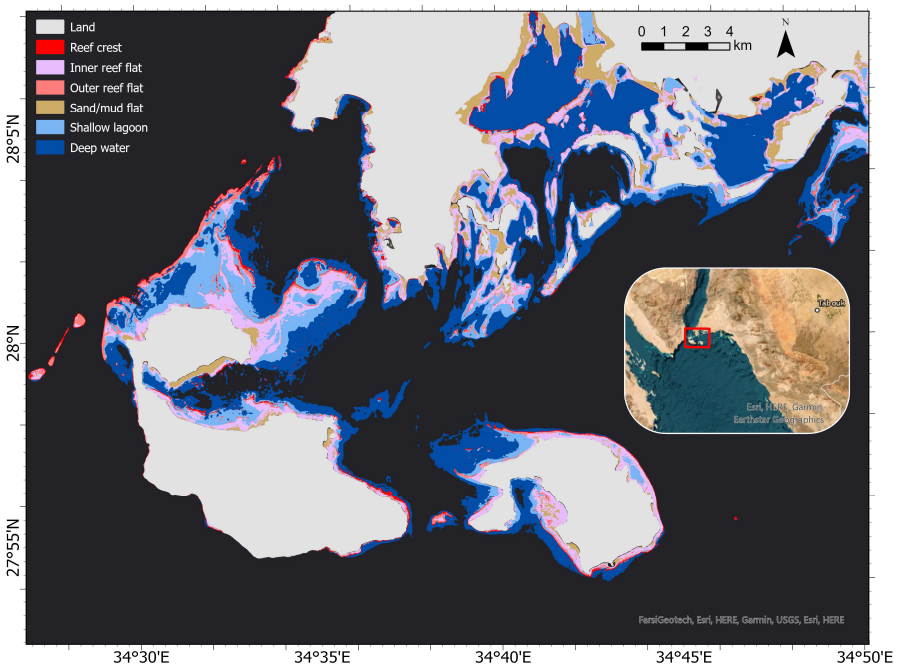


Figure 4. Geomorphic classification map in Sindalah/Strait of Tiran in the NEOM region, Red Sea. The six classes mapped are reef crest, inner and outer reef flat, sand/mud flat, shallow lagoon, and deep water.

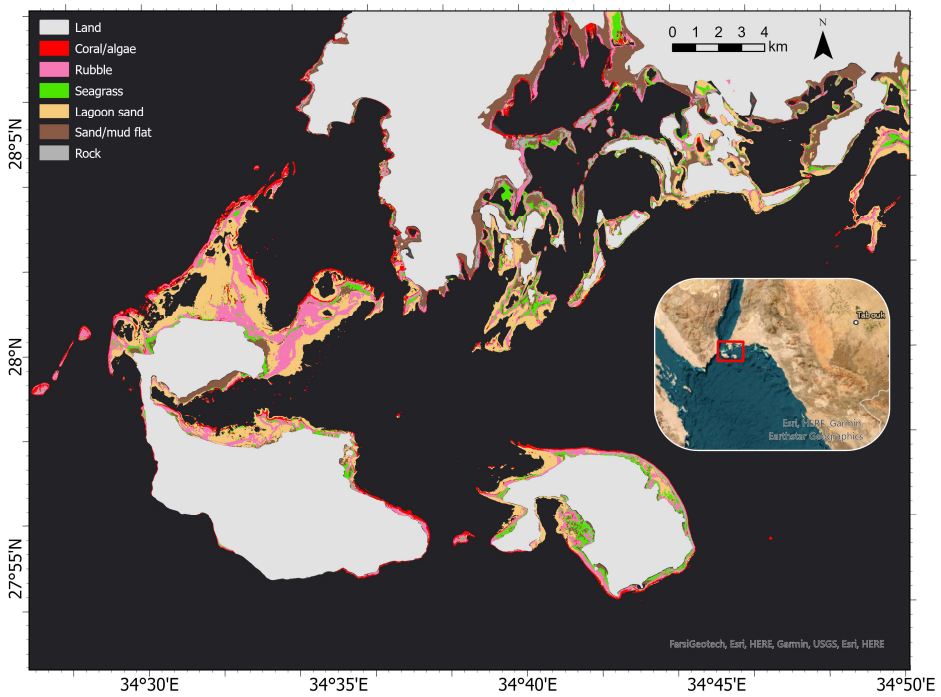


Figure 5. Benthic habitat classification map in Sindalah/Strait of Tiran in the NEOM region, Red Sea. The six benthic classes mapped are coral and dense algae, rubble, seagrass, lagoonal sands, sand/mud flats, and rock (or other hard substrates).

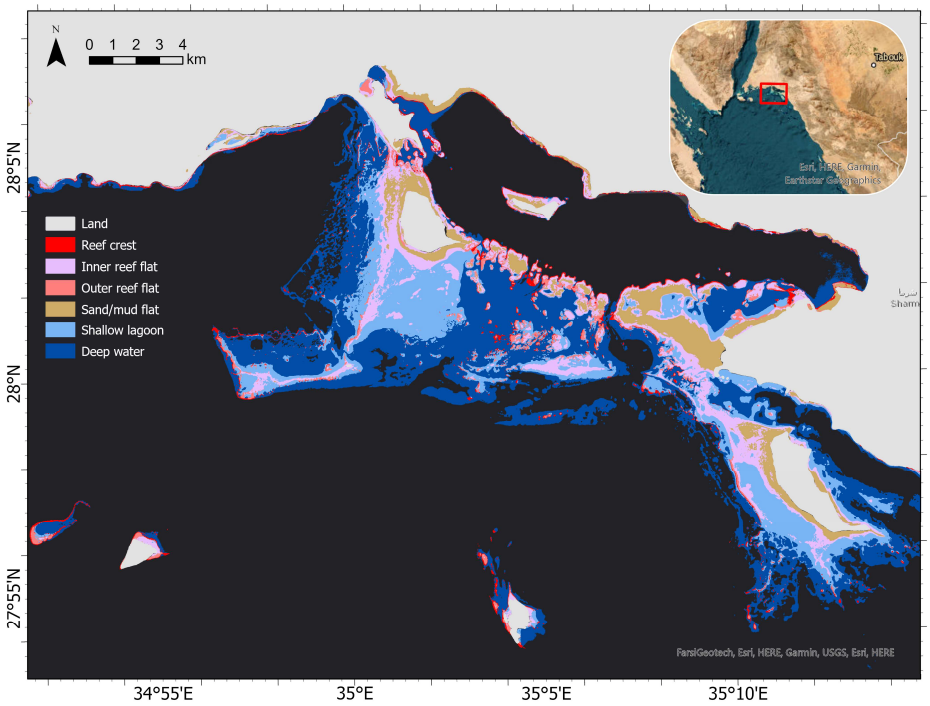


Figure 6. Geomorphic classification map in Sharma, a semi-enclosed tropical lagoon in the NEOM region, Red Sea. The six mapped classes are reef crest, inner and outer reef flat, sand/mud flat, shallow lagoon, and deep water.

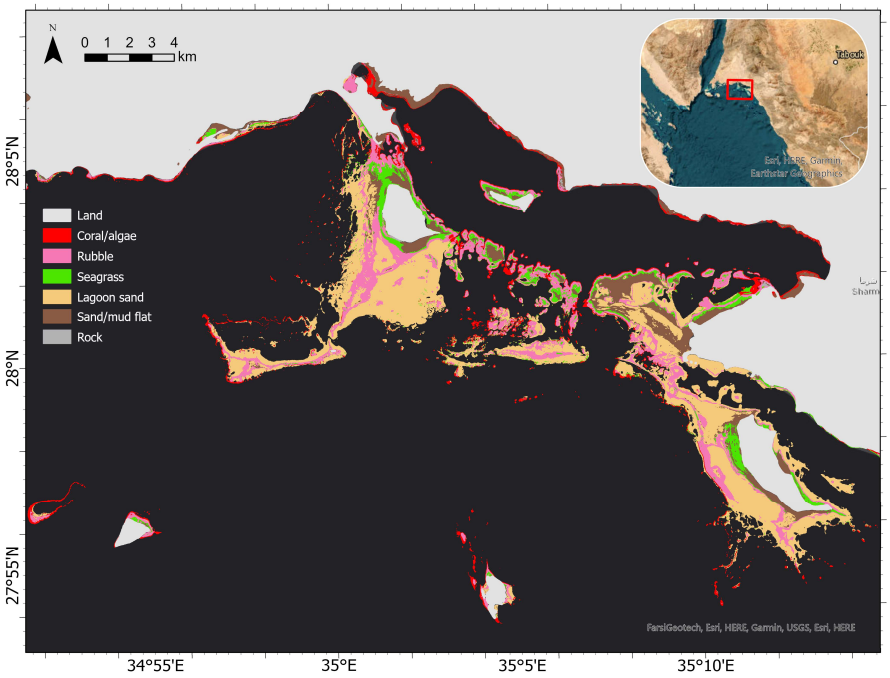


Figure 7. Benthic habitat classification map in Sharma, a semi-enclosed tropical lagoon in the NEOM region, Red Sea. The six benthic classes mapped are coral and dense algae, rubble, seagrass, lagoonal sands, sand/mud flats, and rock (or other hard substrates).

The benthic habitat classification's (Figures 5 and 7) overall accuracy was 73%. The lagoon sand class had the highest producer's accuracy (80% Table 6) and highest user's accuracy (91%). The coral/algae class also performed well, achieving over 70% in both producer's and user's accuracy. The seagrass and rock classes had the lowest producer's accuracies. Seagrass, rubble, and rock reference points were most frequently misclassified

as sand/mud flats (Table 5 and Table S3). The rock and rubble classes had the lowest user's accuracies (51% and 52%, respectively). The class most frequently misclassified as rubble was lagoon sand, and the classes most frequently misclassified as rock were rubble and sand/mud flats (Table 5 and Table S3). The lagoon sand class had the greatest predicted coverage (93.8 km^2), followed by rubble (36.1 km^2), sand/mud flats (34.6 km^2), seagrass (29.2 km^2), and coral/algae (26.3 km^2), while the rock class had the lowest predicted coverage (5.0 km^2).

Table 4. Error matrix populated by proportions of the area for the geomorphic classification in the NEOM region, northern Red Sea (Orf: outer reef flat; Irf: inner reef flat; Rc: reef front and crest; Ls: shallow lagoon; Flt: sand and mud flats; Wtr: deep water). For an error matrix of sample counts, see Supplementary Materials Table S2.

		Reference						
		Orf	**Rc**	**Ls**	**Flt**	**Wtr**	**Irf**	**Pixel Count**
Classified	**Orf**	0.035	0.000	0.014	0.001	0.000	0.013	200,688
	Rc	0.000	0.031	0.012	0.000	0.002	0.005	176,667
	Ls	0.000	0.001	0.148	0.000	0.015	0.001	839,001
	Flt	0.001	0.000	0.000	0.107	0.000	0.019	400,130
	Wtr	0.001	0.003	0.021	0.001	0.282	0.000	2,120,360
	Irf	0.015	0.001	0.023	0.053	0.000	0.195	642,832

Table 5. Error matrix populated by proportions of the area for the benthic habitat classification in the NEOM region, northern Red Sea. For an error matrix of sample counts, see Supplementary Materials Table S3.

		Reference						
		Sand	**Flats**	**Rubble**	**Seagrass**	**Coral/ Algae**	**Rock**	**Pixel Count**
Classified	**Sand**	0.170	0.003	0.003	0.006	0.005	0.000	823,850
	Flats	0.000	0.137	0.021	0.045	0.000	0.008	379,562
	Rubble	0.067	0.032	0.139	0.011	0.013	0.003	515,898
	Seagrass	0.021	0.002	0.002	0.119	0.013	0.000	199,438
	Coral/Algae	0.014	0.005	0.011	0.003	0.083	0.000	273,592
	Rock	0.000	0.011	0.013	0.002	0.006	0.033	57,407

Table 6. Accuracy statistics and estimated areas covered by each class with a ±95% confidence interval (PA = producer's accuracy; UA = user's accuracy).

Geomorphic Classification			**Overall Accuracy**		**84.2 ± 2.2**	
Classes	**Reef Crest**	**Outer Reef Flat**	**Inner Reef Flat**	**Sand/Mud Flat**	**Shallow Lagoon**	**Deep Water**
Area (km^2)	13.9 ± 3.7	15.6 ± 3.5	56.1 ± 5.2	46.6 ± 4.3	103.6 ± 8.2	202.1 ± 7.9
PA (%)	78.6 ± 15.9	71.9 ± 11.6	77.7 ± 5.5	72.3 ± 5.5	72.7 ± 5.2	95.9 ± 1.9
UA (%)	61.7 ± 14.0	55.9 ± 12.8	67.9 ± 5.6	84.2 ± 6.6	89.7 ± 4.8	91.4 ± 3.2
Benthic Habitat Classification			**Overall Accuracy**		**73.0 ± 3.3**	
Classes	Coral/algae	Sand/mud flat	Rock	Rubble	Lagoon sand	Seagrass
Area (km^2)	26.3 ± 4.2	34.6 ± 4.7	5.0 ± 1.8	36.1 ± 5.2	93.8 ± 6.1	29.2 ± 4.6
PA (%)	74.2 ± 9.3	71.4 ± 7.7	58.8 ± 19.2	74.9 ± 7.6	79.7 ± 3.7	52.3 ± 8.1
UA (%)	71.2 ± 10.5	65.2 ± 8.2	51.2 ± 15.5	52.4 ± 7.6	90.7 ± 5.3	76.5 ± 8.4

The benthic maps and class area estimates (Table 6) were compared to previous mapping exercises in the area, the Allen Coral Atlas (version downloaded 20 December

2022 [71]), and JICA and NCWCD 2000. Comparisons of selected areas are shown in Figures 8 and 9, with further examples in Figures S1 and S2 in the Supplementary Materials. In the Allen Coral Atlas, the sand class had the greatest mapped extent calculated in QGIS (148 km^2), followed by rubble (71 km^2), coral/algae (63 km^2), rock (62 km^2), seagrass (23 km^2), and microalgal mats (2 km^2). The total area covered is larger than this study (370 versus 225 km^2), primarily because it extended into deeper water, which is also visible in Figures 8 and 9. The dominant classes from the JICA and NCWCD 2000 classification were as follows: sand with reef patches (106 km^2), and (61 km^2), coral (coverage 11–30%) (59 km^2), turf/small algae (43 km^2), tidal flats (32 km^2), seagrass (31 km^2), coral (coverage 76–100%) (24 km^2), Cyanophycea (11 km^2), coral (coverage 31–50%) (6 km^2), coral (coverage 51–75%) (5 km^2), Sabkah (4 km^2), and macroalgae (0.01 km^2).

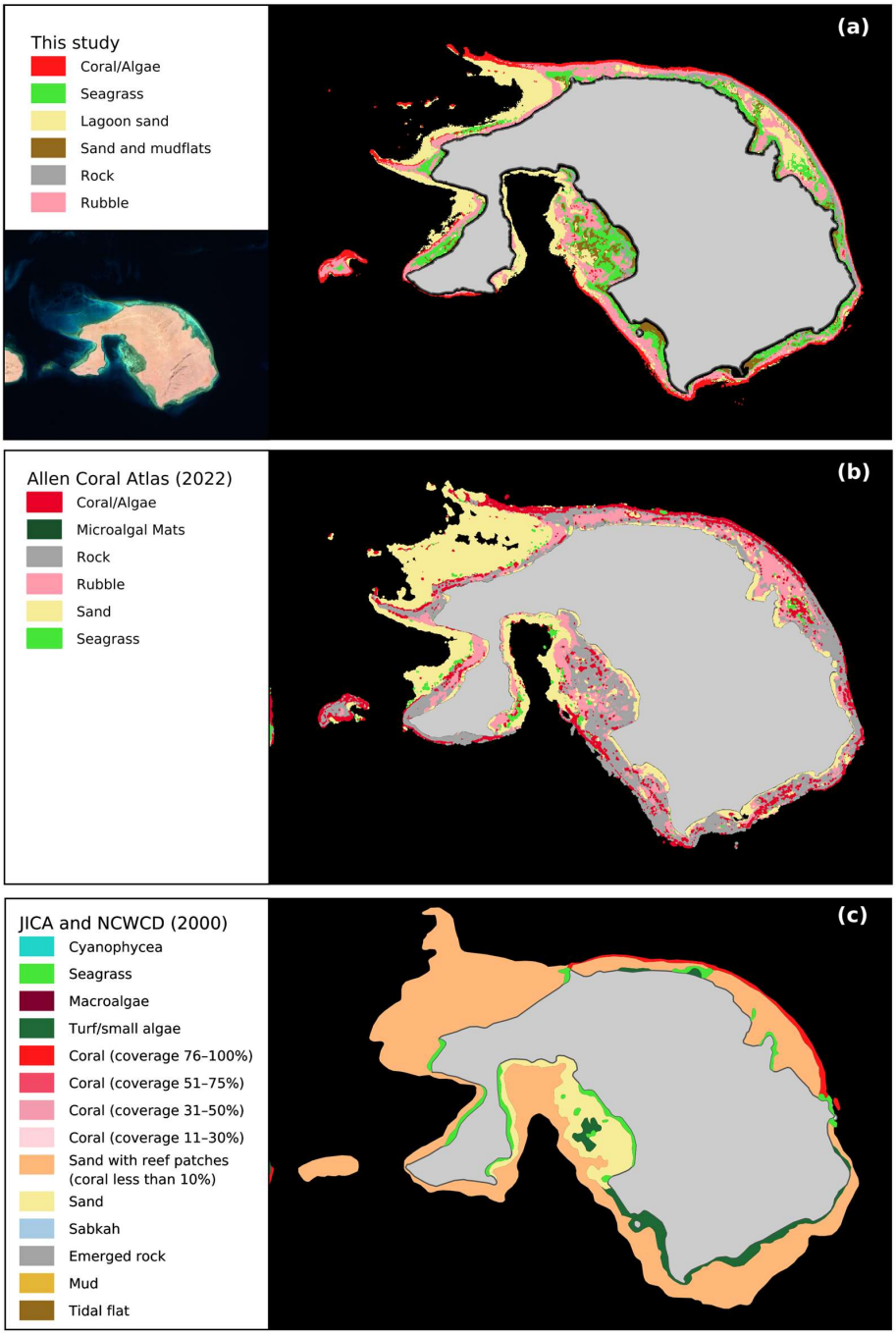


Figure 8. Comparison of three different benthic classification maps covering Sanafir Island, in the northern Red Sea: (**a**) this study, (**b**) Allen Coral Atlas, and (**c**) JICA and NCWCD 2000.

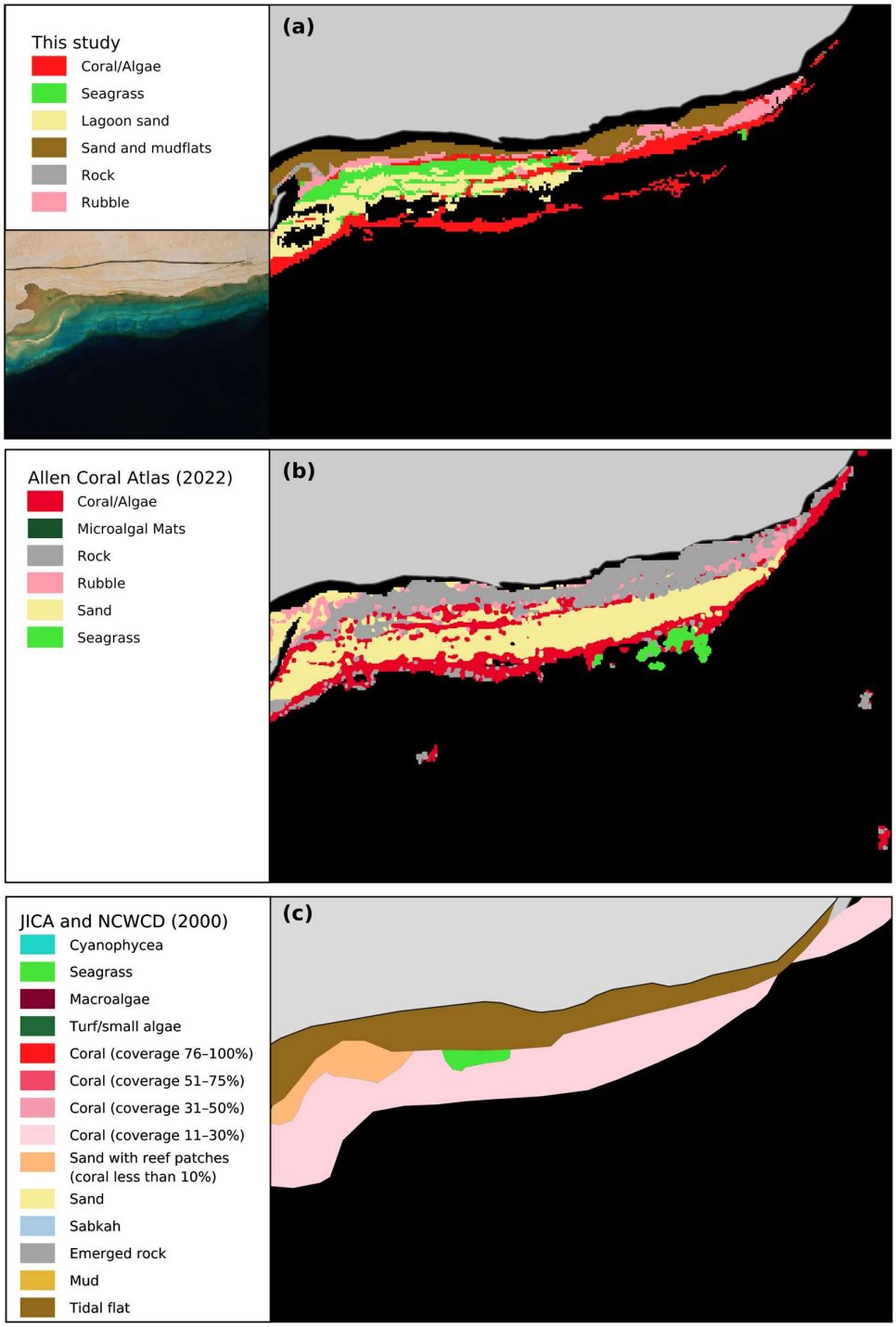


Figure 9. Comparison of three different benthic classification maps for a coastal stretch near Gayal in the NEOM region, Red Sea, showing sills and depressions of reticulated reef structures: (**a**) this study, (**b**) Allen Coral Atlas, and (**c**) JICA and NCWCD 2000.

4. Discussion

Coastal resource management requires reliable and up-to-date spatial data on the distribution of major habitats. Such information is useful in decision-making regarding marine space usage, monitoring the impact of anthropogenic activities, and developing conservation interventions. Despite the global importance of reef systems in the NRS, the region remains relatively understudied. In the context of rapidly increasing temperatures [17,19], extended heat waves [20], and coastal development in the NEOM region, a baseline understanding of the marine environment is crucial. Although there have been

considerable efforts to map coastal habitats in the NRS, these efforts have been limited in their spatial scope, challenging to replicate, or lacking in local validation. Here, we employed remote sensing methods, including UAV and satellite observations, to produce a characterisation of this important region with an associated accuracy assessment and habitat extent estimates. This work contributes to the rapidly increasing body of research focusing on the spatial assessment of marine biodiversity, health status, and environmental pressures in the NEOM area [9,20].

An estimated area of 26.3 km^2 of the study region was covered by coral or dense algae, and 36.1 km^2 was rubble or sparse coral. In total, up to 28% of the shallow coastal environment in the NEOM region were covered by these coral-containing classes, which provide important ecosystem services and biological niches. Corals in the NRS are of global importance due to their high biodiversity and endemism, as well as their high thermal tolerance, making them a potential refuge from global warming [3,5–7,21,22]. They also potentially have significant economic value as they are likely to attract visitors who wish to explore healthy marine ecosystems [10–13]. It is hoped mapping efforts like the one provided in this study will aid conservation managers' decisions to safeguard coral hotspots from the possible impacts of increased maritime traffic, coastal development projects, and unsustainable tourism. The extent of seagrass meadows, an important carbon-capturing habitat in the NRS, was estimated to cover 29.2 km^2 of the study area. Seagrass meadows provide habitats for many organisms, including threatened and endangered species such as dugongs and green turtles. Seagrass meadows are also capable of sequestering significant amounts of carbon and storing it for centuries, even in a low-nutrient, high-respiration environment such as the Red Sea, making them an efficient and cost-effective tool to help the kingdom meet its net-zero emissions target by 2060. Using the extent reported in this study and the average carbon content (3.4 ± 0.3 kg C_{org} m^{-2}) in 1 m thick soil deposits and carbon accumulation rates (6.8 ± 1.7 g C_{org} m^{-2} yr^{-1}) measured in Serrano et al., 2018 [72], we estimate seagrass beds in the NEOM region currently store around 100,000 tonnes of C_{org} and accumulate around 200 tonnes of C_{org} annually. This carbon storage is particularly significant because the terrestrial environment is characterised by arid desert with low C_{org} storage potential [72]. The loss of these habitats not only reduces their carbon sequestration potential but also releases a significant amount of the stored carbon back into the atmosphere [73–75]. Therefore, their conservation should be a priority for the NEOM project in order to meet its environmental goals.

This study is the first to use freely available Sentinel-2 satellite imagery to map coastal habitats on the Saudi Arabian NRS coast. Sentinel-2 MSI has a regular revisit period of ~5 days in a sun-synchronous orbit, which offers consistency over time and therefore has great potential for monitoring. The overall accuracy of both the geomorphic and benthic classifications fall within the range of accuracies reported in other studies that have used Sentinel-2 imagery to map benthic habitats. For example, Poursanidis et al. (2021) [26] classified the Quirimbas National Park in Mozambique into four benthic habitats and obtained an accuracy of 82%. Hamuna et al. (2023) mapped benthic habitats in Kapota Atoll, Wakatobi National Park, Indonesia, using nine classes with 65.3% overall accuracy [76]. Pottier et al. (2021) [77] identified ten benthic habitat classes in the National Park of Banc d'Arguin, Mauritania, with 71.6% overall accuracy when distinguishing between seagrass species and 86.7% without the distinction. However, it is important to note that accuracies reported in different studies could be influenced by the local complexity of the environment, the classification scheme, the validation procedure, and the method of accuracy assessment [36]. Here, we observed a slightly higher accuracy for the geomorphic classification than for the benthic classification, which was anticipated from the results

of the Jeffries–Matusita separability analysis and has been found previously in other reef mapping studies [31,41,78].

The spatial resolution of the Sentinel-2 imagery is sufficient to get an overview of the seabed character; however, benthic habitats exhibit complex and heterogeneous patterns at finer spatial scales. A single 10 × 10 m pixel from Sentinel-2 is often composed of multiple benthic classes, resulting in a mixed spectral signal. In addition, some benthic classes have similar spectral properties, particularly considering relatively few spectral bands are available from multispectral sensors due to attenuation by the water column. These factors make it challenging to separate classes accurately. Here, the overlap between training populations of different classes indicated by JM values < 1.9 suggested that separating these classes without some confusion is unavoidable [67]. As a result, detecting shifts from one class to another is also challenging. The rubble class in particular had low separability scores, which could be due to variations in the proportions of sand, rubble, sparse coral patches, and algae within a single pixel contributing to the signal, and previous studies have suggested the high heterogeneity of this class makes it challenging to map accurately [76].

The habitat maps produced in this study are generally consistent with previous mapping exercises on a large scale (listed in Supplementary Table S1). The use of Sentinel-2 imagery provided a significant improvement in spatial resolution compared to the UNEP-WCMC global distribution of coral reefs [32], which is lower-resolution in this region and excludes some smaller reef areas and reticulated reef networks. Figures 8 and 9 show comparisons between the benthic classification in this study and the two other classifications that cover the entirety of this area: the Allen Coral Atlas [71] and JICA and NCWCD, 2000 [30]. Some features are clearly identifiable in all three products (e.g., a high coral cover reef edge, sand-dominated lagoon areas), but there are notable differences, too. One notable difference is that the Allen Coral Atlas has considerably larger areas of rock compared to this study. The presence of few clear examples of rock substrate compared to the other classes in our training sites limited the available sites for reference points for this class, and it is possible the classification does not capture the diversity of rock areas that may be present in the unseen test sites. However, many of the areas classified as rock along the coast in the Allen Coral Atlas are classified as sand or mud flat in this classification, a class that does not exist in the Allen Coral Atlas, so this may partially explain the difference in rock areas between the two classifications. The total estimated area of seagrass in all three studies is similar (29 km^2 in this study, 23 km^2 in Allen Coral Atlas 2022, 31 km^2 in JICA & NCWCD, 2000); however, as demonstrated in Figures 8 and 9, the distribution can be spatially inconsistent between maps. The study area hosts a number of species of seagrass at varying densities and depths, which makes their classification challenging. The lagoon sand class in particular is widespread and exhibits relatively high levels of confusion with other classes (rubble, seagrass, coral/algae), and we anticipate these areas may also include sparse seagrass and corals in some locations. Seagrass reference points were most frequently misclassified as sand/mud flats, which may be due to similar spectral properties where seagrass was sparse and shallow. The total area of the coral/algae class is significantly lower in this study compared to the Allen Coral Atlas classification (26 km^2 and 63 km^2, respectively), but the percentage of the class compared to the total mapped benthic area is more similar (12% and 17%, respectively). This is explained by the difference in thresholds for deep water, which translates into a significantly larger benthic habitat extent mapped in the Allen Coral Atlas (370 versus 225 km^2). Consequently, deeper coral shelves are excluded in this study but included in Allen Coral Atlas figures. Additionally, the spatial resolution of the input satellite data (10 × 10 m) of this study is likely to result in more 'mixed' pixels that contain coral but that are spectrally dominated by other benthic covers, so they would not be classified as coral, leading to an underestimation of

coral/algae cover. This is particularly apparent in complex areas such as reticulated reef structures, which are found in several locations along the NRS coastline. These structures usually consist of coral filaments 1–10 m across in a honeycomb pattern built on a *Porites* framework, surrounded by sand and rubble [1,3], and they are only partially captured in the current classification because of their narrow width compared to a pixel footprint (Figure 9). This demonstrates that while Sentinel-2 is appropriate for characterising the benthic environment at the regional level, it is important to acknowledge the trade-offs with resolution, and as such, different techniques may be needed for users wishing to refine maps of specific sites of interest.

Recommendations

A key objective of this study was to develop a methodology that would be accessible and repeatable for large areas, using freely-available software and satellite imagery. One of the challenges in many mapping exercises, particularly those in remote and/or understudied areas, is the availability of ground-truth data. Therefore, UAV surveys were used as an alternative to traditional boat-based or snorkel surveys to collect data above water over large areas. This proved to be an efficient method for collecting information over a range of sites, covering a much larger area than would have been possible with underwater surveys in the available time. However, in some instances, the ripples caused by wind on the water's surface prevented the accurate determination of the bottom type, leading to the exclusion of affected validation points. Even when wind was not a factor, it was sometimes challenging to assign a class to the bottom cover, even in the very-high resolution imagery. To address this issue, we recommend conducting UAV surveys in conjunction with underwater surveys to provide more detailed information on benthic cover and establish a direct link between remotely-observed images and the seabed. The training and validation sites for this study were limited to selected areas off the mainland coast, chosen based on an initial classification to represent a diversity of habitats. While the accuracy is reported for the entire area, it is important to note that differences in reef structure, communities, and water quality may cause the accuracy to vary when applied to offshore reef areas. Previous research has shown that classification accuracy can decrease when applied away from training sites [66]. Therefore, we recommend ongoing investment in collecting and sharing in situ data in these environments to ensure the representativeness of this work and enable testing future classifiers across reef types.

In addition to underwater in situ data, the habitat maps in this area potentially could be improved with the addition of environmental data, such as high-resolution bathymetry and wave exposure, and higher-resolution optical imagery [65]. For example, high-quality bathymetry data collected or derived from satellites can enable the calculation of slope and rugosity, which may help distinguish benthic composition based on their environmental niches [65,79]. Additionally, bathymetry can assist in masking areas outside of reasonable detection limits. Radiative transfer modelling has demonstrated that even in clear coral reef waters, dark substrates such as corals have a depth-of-detection limit on the order of 10–20 m [80]. The use of commercial high-resolution imagery, such as Planet Scope or WorldView-3, is increasingly popular for benthic mapping, particularly over small study areas [29,79,81,82]. Recent studies have shown higher-resolution imagery can provide more detailed maps and potentially improve the accuracy of benthic classification, particularly in fragmented areas [42,83]. Therefore, future work could explore using high-resolution imagery in complex areas such as reticulated reef structures or consider data fusion to take advantage of the spatial resolution of high-resolution imagery with the spectral resolution of Sentinel-2 [84].

5. Conclusions

This study demonstrated the ability to use training data derived from UAV imagery, in combination with freely-available satellite data from Sentinel-2, to classify benthic cover in a diverse tropical sea using the Random Forest machine learning algorithm. This was the first study to generate a map of the NEOM area using Sentinel-2 data, mapping 225 km^2 of underwater habitats visible from space. Two levels of classification were conducted, one based on geomorphic characteristics and the other on benthic habitat type, each comprising six distinct classes. The classification outputs provide information about the coastal benthic habitats of the NEOM region, valuable for marine conservation at a pivotal time when several coastal projects are commencing and climate pressures from rising ocean temperatures and more frequent heatwave events are mounting. In particular, coral or dense algae, a globally important habitat that supports reef species diversity, endemic species, and biomass, was estimated to cover an area of 26.3 km^2. Seagrass beds were estimated to cover approximately 29.2 km^2 and may sequester around 200 tonnes of C_{org} annually, highlighting their importance in climate regulation as well as their role as a crucial habitat for marine life. Information on the location and extent of these benthic habitats is expected to help guide effective management strategies and associated protection and restoration efforts.

Anthropogenic activities, particularly coastal development, can have a significant impact on marine habitats and potentially lead to changes in ecosystem dynamics, the consequences of which are not fully understood. To avoid potential ecological damage, stakeholders should consider the distribution of marine habitats when planning coastal projects. Monitoring the distribution and health of marine habitats before, during, and after the construction of these projects should also be prioritised. The authors recommend continued investment in the collection and sharing of in situ data such as UAV and underwater surveys in key locations along the Red Sea coastline. Such data enable the monitoring of local ecosystem health and can further improve the development and validation of habitat maps based on remote sensing approaches.

This study demonstrated an accessible, replicable workflow for coastal habitat mapping in challenging environments such as the NRS. While the methods used in this study are well established, the maps provide a foundation for ongoing work in this region by providing a baseline classification for comparison and targeting future studies. The results highlight the persistent challenge of mixed pixels and spectral similarity between classes at different depths in benthic classification using moderate-resolution imagery, while helping to identify which classes and locations are most affected. These findings motivate future work on spectral unmixing techniques and sub-pixel classification approaches, which use the spectral signatures of each class to estimate their proportion within a pixel. The use of additional datasets, such as high-resolution bathymetry, and further investigation of the theoretical relationships between water depth, substrate type, and remote sensing reflectance will further help define detection limits and improve map accuracy. This study also identified areas of development specific for the NRS, such as the need to improve the characterisation of narrow reticulated reef networks, potentially through the use of higher-resolution imagery or data fusion between Sentinel-2 and higher-resolution platforms. Addressing these theoretical and methodological challenges will contribute to the refinement of coastal habitat mapping techniques, enabling more accurate mapping to support conservation and management efforts in complex benthic environments, like the NRS.

Supplementary Materials: The following supporting information can be downloaded at: https://www.mdpi.com/article/10.3390/rs17030485/s1, Table S1: A brief description and visualisation of existing global and regional benthic cover and coral and seagrass extent datasets available in the northern Red Sea; Table S2: Error matrix and classification accuracy from sample counts for the geomorphic classification in the NEOM region, northern Red Sea; Table S3: Error matrix and classification accuracy from sample counts for the benthic habitat classification in the NEOM region, northern Red Sea; Figure S1: Comparison maps of benthic habitat classifications covering a stretch of the northwest coast of Ras Alsheikh Hamid, Gulf of Aqaba; Figure S2: Comparison maps of benthic habitat classifications covering Tiran Island, northern Red Sea.

Author Contributions: Conceptualisation, E.S., N.P. and D.C.; Data curation, E.S. and N.P.; Formal analysis, E.S. and N.P.; Funding acquisition, S.G., D.E.R. and I.H.; Investigation, N.P.; Methodology, E.S. and N.P.; Project administration, S.G., D.E.R. and I.H.; Resources, S.G., D.E.R. and I.H.; Software, E.S., N.P. and D.C.; Supervision, S.G., D.E.R. and I.H.; Validation, E.S. and N.P.; Visualisation, E.S. and N.P.; Writing—original draft, E.S. and N.P.; Writing—review and editing, D.C., S.G., D.E.R. and I.H. All authors have read and agreed to the published version of the manuscript.

Funding: This research was funded by the Virtual Red Sea Initiative, with grant number REP/1/3268-01-01, and the KAUST Center of Excellence for NEOM.

Data Availability Statement: Data are available upon request due to restrictions imposed by agreements with the project funders. The other classifications mentioned in this manuscript (The Allen Coral Atlas and the JICA and NCWCD 2000) can be obtained from their respective creators.

Acknowledgments: We would like to thank the UAV operators from the Shamal Group, for their work collecting the drone survey data in remote locations in a short period of time, sharing their knowledge about the study area, and communicating with the local authorities regarding the flight permits. We thank ESA and the Copernicus programme for providing access to the Sentinel-2 data archive. We would also like to acknowledge the creators and maintainers of ACOLITE software and RSGISLib python library which facilitated the pre-processing and classification work in this study. We acknowledge the NERC Earth Observation Data Analysis and AI Service (NEODAAS) for the use of computing resources.

Conflicts of Interest: The authors declare no conflicts of interest.

References

1. Bruckner, A.W.; Rowlands, G.; Riegl, B.; Purkis, S.; Williams, A.; Renaud, P.G. *Khaled Bin Sultan Living Oceans Foundation Atlas of Saudi Arabian Red Sea Marine Habitats*, 2nd ed.; Panoramic Press: Landover, MD, USA, 2012; ISBN 978-0-9835611-1-8.
2. Gladstone, W.; Tawfiq, N.; Nasr, D.; Andersen, I.; Cheung, C.; Drammeh, H.; Krupp, F.; Lintner, S. Sustainable Use of Renewable Resources and Conservation in the Red Sea and Gulf of Aden: Issues, Needs and Strategic Actions. *Ocean Coast. Manag.* **1999**, *42*, 671–697. [CrossRef]
3. DeVantier, L.; Turak, E.; Al-Shaikh, K.; De'ath, G. Coral Communities of the Central-Northern Saudi Arabian Red Sea. *Fauna Arab.* **2000**, *18*, 23–66.
4. DiBattista, J.D.; Howard Choat, J.; Gaither, M.R.; Hobbs, J.-P.A.; Lozano-Cortés, D.F.; Myers, R.F.; Paulay, G.; Rocha, L.A.; Toonen, R.J.; Westneat, M.W.; et al. On the Origin of Endemic Species in the Red Sea. *J. Biogeogr.* **2016**, *43*, 13–30. [CrossRef]
5. Kleinhaus, K.; Al-Sawalmih, A.; Barshis, D.J.; Genin, A.; Grace, L.N.; Hoegh-Guldberg, O.; Loya, Y.; Meibom, A.; Osman, E.O.; Ruch, J.-D.; et al. Science, Diplomacy, and the Red Sea's Unique Coral Reef: It's Time for Action. *Front. Mar. Sci.* **2020**, *7*, 90. [CrossRef]
6. Fine, M.; Cinar, M.; Voolstra, C.R.; Safa, A.; Rinkevich, B.; Laffoley, D.; Hilmi, N.; Allemand, D. Coral Reefs of the Red Sea—Challenges and Potential Solutions. *Reg. Stud. Mar. Sci.* **2019**, *25*, 100498. [CrossRef]
7. Terraneo, T.I.; Ouhssain, M.; Castano, C.B.; Aranda, M.; Hume, B.C.C.; Marchese, F.; Vimercati, S.; Chimienti, G.; Eweida, A.A.; Voolstra, C.R.; et al. From the Shallow to the Mesophotic: A Characterization of Symbiodiniaceae Diversity in the Red Sea NEOM Region. *Front. Mar. Sci.* **2023**, *10*, 1077805. [CrossRef]
8. Kochman-Gino, N.-R.; Fine, M. Reef Building Corals Show Resilience to the Hottest Marine Heatwave on Record in the Gulf of Aqaba. *Front. Mar. Sci.* **2023**, *10*, 1215567. [CrossRef]

9. Papagiannopoulos, N.; Raitsos, D.E.; Krokos, G.; Gittings, J.A.; Brewin, R.J.W.; Papadopoulos, V.P.; Pavlidou, A.; Selmes, N.; Groom, S.; Hoteit, I. Phytoplankton Biomass and the Hydrodynamic Regime in NEOM, Red Sea. *Remote Sens.* **2021**, *13*, 2082. [CrossRef]
10. Beaumont, N.J.; Austen, M.C.; Mangi, S.C.; Townsend, M. Economic Valuation for the Conservation of Marine Biodiversity. *Mar. Pollut. Bull.* **2008**, *56*, 386–396. [CrossRef]
11. Pearce, D.W. The Value of Biodiversity. In *Microbial Diversity and Bioprospecting*; ASM Press: Washington, DC, USA, 2003; pp. 469–475. ISBN 978-1-68367-217-3.
12. Rees, S.E.; Rodwell, L.D.; Attrill, M.J.; Austen, M.C.; Mangi, S.C. The Value of Marine Biodiversity to the Leisure and Recreation Industry and Its Application to Marine Spatial Planning. *Mar. Policy* **2010**, *34*, 868–875. [CrossRef]
13. Turpie, J.K.; Heydenrych, B.J.; Lamberth, S.J. Economic Value of Terrestrial and Marine Biodiversity in the Cape Floristic Region: Implications for Defining Effective and Socially Optimal Conservation Strategies. *Biol. Conserv.* **2003**, *112*, 233–251. [CrossRef]
14. Intergovernmental Panel on Climate Change (IPCC). *Climate Change 2022–Impacts, Adaptation and Vulnerability: Working Group II Contribution to the Sixth Assessment Report of the Intergovernmental Panel on Climate Change*, 1st ed.; Cambridge University Press: Cambridge, UK, 2023; ISBN 978-1-00-932584-4.
15. Burke, L.; Reytar, K.; Spadling, M.; Perry, A. *Reefs at Risk–Revisited*; World Resource Institute report; World Resources Institute: Washington, DC, USA, 2011; ISBN 978-1-56973-762-0.
16. Carvalho, S.; Kürten, B.; Krokos, G.; Hoteit, I.; Ellis, J. The Red Sea. In *World Seas: An Environmental Evaluation*, 2nd ed.; Elsevier: Amsterdam, The Netherlands, 2019; pp. 49–74.
17. Chaidez, V.; Dreano, D.; Agusti, S.; Duarte, C.M.; Hoteit, I. Decadal Trends in Red Sea Maximum Surface Temperature. *Sci. Rep.* **2017**, *7*, 8144. [CrossRef] [PubMed]
18. Krokos, G.; Papadopoulos, V.; Sofianos, S.; Obao, H.; Dybczak, P.; Hoteit, I. Natural Climate Oscillations May Counteract Red Sea Warming over the Coming Decades. *Geophys. Res. Lett.* **2019**, *46*, 454–3461. [CrossRef]
19. Raitsos, D.E.; Hoteit, I.; Prihartato, P.K.; Chronis, T.; Triantafyllou, G.; Abualnaja, Y. Abrupt Warming of the Red Sea. *Geophys. Res. Lett.* **2011**, *38*, 47984. [CrossRef]
20. Genevier, L.G.C.; Jamil, T.; Raitsos, D.E.; Krokos, G.; Hoteit, I. Marine Heatwaves Reveal Coral Reef Zones Susceptible to Bleaching in the Red Sea. *Glob. Change Biol.* **2019**, *25*, 2338–2351. [CrossRef]
21. Fine, M.; Gildor, H.; Genin, A. A Coral Reef Refuge in the Red Sea. *Glob. Change Biol.* **2013**, *19*, 3640–3647. [CrossRef]
22. Osman, E.O.; Smith, D.J.; Ziegler, M.; Kürten, B.; Conrad, C.; El-Haddad, K.M.; Voolstra, C.R.; Suggett, D.J. Thermal Refugia against Coral Bleaching throughout the Northern Red Sea. *Glob. Change Biol.* **2018**, *24*, e474–e484. [CrossRef]
23. Farag, A. The Story of NEOM City: Opportunities and Challenges. In *New Cities and Community Extensions in Egypt and the Middle East: Visions and Challenges*; Attia, S., Shafik, Z., Ibrahim, A., Eds.; Springer: Cham, Switzerland, 2019; pp. 35–49. ISBN 978-3-319-77874-7.
24. Grand, S.; Wolff, K. *Assessing Saudi Vision 2030: A 2020 Review*; Atlantic Council: Washington, DC, USA, 2020; Volume 17.
25. The Future of Nature. Available online: https://www.neom.com/en-us/nature (accessed on 5 January 2024).
26. Poursanidis, D.; Traganos, D.; Teixeira, L.; Shapiro, A.; Muaves, L. Cloud-native Seascape Mapping of Mozambique's Quirimbas National Park with Sentinel-2. *Remote Sens. Ecol. Conserv.* **2021**, *7*, 275–291. [CrossRef]
27. Roff, J.C.; Taylor, M.E.; Laughren, J. Geophysical Approaches to the Classification, Delineation and Monitoring of Marine Habitats and Their Communities. *Aquat. Conserv. Mar. Freshw. Ecosyst.* **2003**, *13*, 77–90. [CrossRef]
28. Foo, S.A.; Asner, G.P. Scaling Up Coral Reef Restoration Using Remote Sensing Technology. *Front. Mar. Sci.* **2019**, *6*, 79. [CrossRef]
29. Hedley, J.; Roelfsema, C.; Chollett, I.; Harborne, A.; Heron, S.; Weeks, S.; Skirving, W.; Strong, A.; Eakin, C.; Christensen, T.; et al. Remote Sensing of Coral Reefs for Monitoring and Management: A Review. *Remote Sens.* **2016**, *8*, 118. [CrossRef]
30. JICA; NCWCD. *The Study on Coastal/Marine Habitat and Biological Inventories in the Northern Part of the Red Sea Coast in the Kingdom of Saudi Arabia*; JICA & NCWCD: Riyadh, Saudi Arabia, 2000.
31. Lyons, M.B.; Roelfsema, C.M.; Kennedy, E.; Kovacs, E.; Borrego-Acevedo, R.; Markey, K.; Roe, M.; Yuwono, D.M.; Harris, D.L.; Phinn, S.R.; et al. Mapping the World's Coral Reefs Using a Global Multiscale Earth Observation Framework. *Remote Sens. Ecol. Conserv.* **2020**, *6*, 557–568. [CrossRef]
32. Global Distribution of Warm-Water Coral Reefs, Compiled from Multiple Sources Including the Millennium Coral Reef Mapping Project. 2021. Available online: https://data.unep-wcmc.org/pdfs/1/WCMC_008_Global_Distribution_of_Coral_Reefs.pdf?1617121809 (accessed on 20 November 2024).
33. Global Distribution of Seagrasses (Version 6.0), 2017 SIXTH Update to the Data Layer Used in Green and Short (2003). Available online: https://www.unep-wcmc.org/en (accessed on 20 November 2024).
34. Jayathilake, D.R.M.; Costello, M.J. A modelled global distribution of the seagrass biome. *Biol. Conserv.* **2018**, *226*, 120–126. [CrossRef]
35. Li, J.; Knapp, D.E.; Fabina, N.S.; Kennedy, E.V.; Larsen, K.; Lyons, M.B.; Murray, N.J.; Phinn, S.R.; Roelfsema, C.M.; Asner, G.P. A Global Coral Reef Probability Map Generated Using Convolutional Neural Networks. *Coral Reefs* **2020**, *39*, 1805–1815. [CrossRef]

36. Misiuk, B.; Brown, C.J. Benthic Habitat Mapping: A Review of Three Decades of Mapping Biological Patterns on the Seafloor. *Estuar. Coast. Shelf Sci.* **2024**, *296*, 108599. [CrossRef]
37. Kutser, T.; Hedley, J.; Giardino, C.; Roelfsema, C.; Brando, V.E. Remote Sensing of Shallow Waters–A 50 Year Retrospective and Future Directions. *Remote Sens. Environ.* **2020**, *240*, 111619. [CrossRef]
38. Chennu, A.; Färber, P.; De'ath, G.; De Beer, D.; Fabricius, K.E. A Diver-Operated Hyperspectral Imaging and Topographic Surveying System for Automated Mapping of Benthic Habitats. *Sci. Rep.* **2017**, *7*, 7122. [CrossRef]
39. Nababan, B.; Mastu, L.O.K.; Idris, N.H.; Panjaitan, J.P. Shallow-Water Benthic Habitat Mapping Using Drone with Object Based Image Analyses. *Remote Sens.* **2021**, *13*, 4452. [CrossRef]
40. Monteiro, J.G.; Jiménez, J.L.; Gizzi, F.; Přikryl, P.; Lefcheck, J.S.; Santos, R.S.; Canning-Clode, J. Novel Approach to Enhance Coastal Habitat and Biotope Mapping with Drone Aerial Imagery Analysis. *Sci. Rep.* **2021**, *11*, 574. [CrossRef]
41. Roelfsema, C.; Phinn, S.; Jupiter, S.; Comley, J.; Albert, S. Mapping Coral Reefs at Reef to Reef-System Scales, 10s–1000s Km2, Using Object-Based Image Analysis. *Int. J. Remote Sens.* **2013**, *34*, 6367–6388. [CrossRef]
42. Marcello, J.; Eugenio, F.; Gonzalo-Martin, C.; Rodriguez-Esparragon, D.; Marques, F. Advanced Processing of Multiplatform Remote Sensing Imagery for the Monitoring of Coastal and Mountain Ecosystems. *IEEE Access* **2021**, *9*, 6536–6549. [CrossRef]
43. Rende, S.F.; Bosman, A.; Di Mento, R.; Bruno, F.; Lagudi, A.; Irving, A.D.; Dattola, L.; Giambattista, L.D.; Lanera, P.; Proietti, R.; et al. Ultra-High-Resolution Mapping of *Posidonia Oceanica* (L.) Delile Meadows through Acoustic, Optical Data and Object-Based Image Classification. *J. Mar. Sci. Eng.* **2020**, *8*, 647. [CrossRef]
44. Andréfouët, S.; Bionaz, O. Lessons from a Global Remote Sensing Mapping Project. A Review of the Impact of the Millennium Coral Reef Mapping Project for Science and Management. *Sci. Total Environ.* **2021**, *776*, 145987. [CrossRef]
45. Hedley, J.D.; Roelfsema, C.; Brando, V.; Giardino, C.; Kutser, T.; Phinn, S.; Mumby, P.J.; Barrilero, O.; Laporte, J.; Koetz, B. Coral Reef Applications of Sentinel-2: Coverage, Characteristics, Bathymetry and Benthic Mapping with Comparison to Landsat 8. *Remote Sens. Environ.* **2018**, *216*, 598–614. [CrossRef]
46. Immordino, F.; Barsanti, M.; Candigliota, E.; Cocito, S.; Delbono, I.; Peirano, A. Application of Sentinel-2 Multispectral Data for Habitat Mapping of Pacific Islands: Palau Republic (Micronesia, Pacific Ocean). *J. Mar. Sci. Eng.* **2019**, *7*, 316. [CrossRef]
47. Traganos, D.; Reinartz, P. Mapping Mediterranean Seagrasses with Sentinel-2 Imagery. *Mar. Pollut. Bull.* **2018**, *134*, 197–209. [CrossRef]
48. Traganos, D.; Lee, C.B.; Blume, A.; Poursanidis, D.; Čižmek, H.; Deter, J.; Mačić, V.; Montefalcone, M.; Pergent, G.; Pergent-Martini, C.; et al. Spatially Explicit Seagrass Extent Mapping Across the Entire Mediterranean. *Front. Mar. Sci.* **2022**, *9*, 871799. [CrossRef]
49. Wicaksono, P.; Fauzan, M.A.; Asta, S.G.W. Assessment of Sentinel-2A Multispectral Image for Benthic Habitat Composition Mapping. *IET Image Process.* **2020**, *14*, 279–288. [CrossRef]
50. Wicaksono, P.; Hafizt, M.; Harahap, S.D.; Nandika, M.R. Integrating Sentinel-2 and PlanetScope Image with Drone-Based Seagrass Data for Seagrass Percent Cover Mapping. *IOP Conf. Ser. Earth Environ. Sci.* **2024**, *1291*, 012012. [CrossRef]
51. Bruckner, A.W.; Dempsey, A.C. The Status, Threats, and Resilience of Reef-Building Corals of the Saudi Arabian Red Sea. In *The Red Sea*; Rasul, N.M.A., Stewart, I.C.F., Eds.; Springer Earth System Sciences; Springer: Berlin/Heidelberg, Germany, 2015; pp. 471–486. ISBN 978-3-662-45200-4.
52. Berumen, M.L.; Hoey, A.S.; Bass, W.H.; Bouwmeester, J.; Catania, D.; Cochran, J.E.M.; Khalil, M.T.; Miyake, S.; Mughal, M.R.; Spaet, J.L.Y.; et al. The Status of Coral Reef Ecology Research in the Red Sea. *Coral Reefs* **2013**, *32*, 737–748. [CrossRef]
53. Raitsos, D.E.; Pradhan, Y.; Brewin, R.J.W.; Stenchikov, G.; Hoteit, I. Remote Sensing the Phytoplankton Seasonal Succession of the Red Sea. *PLoS ONE* **2013**, *8*, e64909. [CrossRef] [PubMed]
54. Caballero, I.; Stumpf, R.P. Retrieval of Nearshore Bathymetry from Sentinel-2A and 2B Satellites in South Florida Coastal Waters. *Estuar. Coast. Shelf Sci.* **2019**, *226*, 106277. [CrossRef]
55. Vanhellemont, Q. Adaptation of the Dark Spectrum Fitting Atmospheric Correction for Aquatic Applications of the Landsat and Sentinel-2 Archives. *Remote Sens. Environ.* **2019**, *225*, 175–192. [CrossRef]
56. Vanhellemont, Q.; Ruddick, K. Atmospheric Correction of Metre-Scale Optical Satellite Data for Inland and Coastal Water Applications. *Remote Sens. Environ.* **2018**, *216*, 586–597. [CrossRef]
57. Nurlidiasari, M.; Budhiman, S. Mapping Coral Reef Habitat with and without Water Column Correction Using Quickbird Image. *Int. J. Remote Sens. Earth Sci. IJReSES* **2005**, *2*, 45–56. [CrossRef]
58. Siregar, V.P.; Agus, S.B.; Subarno, T.; Prabowo, N.W. Mapping Shallow Waters Habitats Using OBIA by Applying Several Approaches of Depth Invariant Index in North Kepulauan Seribu. *IOP Conf. Ser. Earth Environ. Sci.* **2018**, *149*, 012052. [CrossRef]
59. Lyzenga, D.R. Remote Sensing of Bottom Reflectance and Water Attenuation Parameters in Shallow Water Using Aircraft and Landsat Data. *Int. J. Remote Sens.* **1981**, *2*, 71–82. [CrossRef]
60. Kennedy, E.; Roelfsema, C.; Lyons, M.; Kovacs, E.; Borrego-Acevedo, R.; Roe, M.; Phinn, S.; Larsen, K.; Murray, N.; Yuwono, D.; et al. Reef Cover: A Coral Reef Classification to Guide Global Habitat Mapping from Remote Sensing. *Sci Data* **2021**, *8*, 196. [CrossRef]

61. Andréfouët, S.; Rilwan, Y.; Hamel, M. Habitat Mapping for Conservation Planning in Baa Atoll, Republic of Maldives. *Atoll Res. Bull.* **2012**, *590*, 207–222.
62. Riegl, B.M.; Bruckner, A.W.; Rowlands, G.P.; Purkis, S.J.; Renaud, P. Red Sea Coral Reef Trajectories over 2 Decades Suggest Increasing Community Homogenization and Decline in Coral Size. *PLoS ONE* **2012**, *7*, e38396. [CrossRef]
63. Bunting, P.; Clewley, D.; Lucas, R.M.; Gillingham, S. The Remote Sensing and GIS Software Library (RSGISLib). *Comput. Geosci.* **2014**, *62*, 216–226. [CrossRef]
64. Pedregosa, F.; Varoquaux, G.; Gramfort, A.; Michel, V.; Thirion, B.; Grisel, O.; Blondel, M.; Prettenhofer, P.; Weiss, R.; Dubourg, V.; et al. Scikit-Learn: Machine Learning in Python. *J. Mach. Learn. Res.* **2011**, *12*, 2825–2830.
65. Nguyen, T.; Liquet, B.; Mengersen, K.; Sous, D. Mapping of Coral Reefs with Multispectral Satellites: A Review of Recent Papers. *Remote Sens.* **2021**, *13*, 4470. [CrossRef]
66. Wicaksono, P.; Aryaguna, P.A.; Lazuardi, W. Benthic Habitat Mapping Model and Cross Validation Using Machine-Learning Classification Algorithms. *Remote Sens.* **2019**, *11*, 1279. [CrossRef]
67. Wicaksono, P.; Aryaguna, P.A. Analyses of Inter-Class Spectral Separability and Classification Accuracy of Benthic Habitat Mapping Using Multispectral Image. *Remote Sens. Appl. Soc. Environ.* **2020**, *19*, 100335. [CrossRef]
68. Richards, J.A. *Remote Sensing Digital Image Analysis*; Springer: Berlin/Heidelberg, Germany, 2013; ISBN 978-3-642-30061-5.
69. Olofsson, P.; Foody, G.M.; Herold, M.; Stehman, S.V.; Woodcock, C.E.; Wulder, M.A. Good Practices for Estimating Area and Assessing Accuracy of Land Change. *Remote Sens. Environ.* **2014**, *148*, 42–57. [CrossRef]
70. FAO. *Map Accuracy Assessment and Area Estimation: A Practical Guide*; National Forest Monitoring Assessment Working Paper No.46/E; FAO: Rome, Italy, 2016.
71. Allen Coral Atlas Imagery, Maps and Monitoring of the World's Tropical Coral Reefs. 2022. Available online: https://allencoralatlas.org/ (accessed on 20 November 2024).
72. Serrano, O.; Almahasheer, H.; Duarte, C.M.; Irigoien, X. Carbon Stocks and Accumulation Rates in Red Sea Seagrass Meadows. *Sci. Rep.* **2018**, *8*, 15037. [CrossRef]
73. Duarte, C.M.; Marbà, N.; Gacia, E.; Fourqurean, J.W.; Beggins, J.; Barrón, C.; Apostolaki, E.T. Seagrass Community Metabolism: Assessing the Carbon Sink Capacity of Seagrass Meadows. *Glob. Biogeochem. Cycles* **2010**, *24*, GB4032. [CrossRef]
74. Fourqurean, J.W.; Duarte, C.M.; Kennedy, H.; Marbà, N.; Holmer, M.; Mateo, M.A.; Apostolaki, E.T.; Kendrick, G.A.; Krause-Jensen, D.; McGlathery, K.J.; et al. Seagrass Ecosystems as a Globally Significant Carbon Stock. *Nat. Geosci.* **2012**, *5*, 505–509. [CrossRef]
75. Pendleton, L.; Donato, D.C.; Murray, B.C.; Crooks, S.; Jenkins, W.A.; Sifleet, S.; Craft, C.; Fourqurean, J.W.; Kauffman, J.B.; Marbà, N.; et al. Estimating Global "Blue Carbon" Emissions from Conversion and Degradation of Vegetated Coastal Ecosystems. *PLoS ONE* **2012**, *7*, e43542. [CrossRef]
76. Hamuna, B.; Pujiyati, S.; Gaol, J.L.; Hestirianoto, T. Spatial Distribution of Benthic Habitats in Kapota Atoll (Wakatobi National Park, Indonesia) Using Remote Sensing Imagery. *Biodiversitas* **2023**, *24*, 3700–3707. [CrossRef]
77. Pottier, A.; Catry, T.; Trégarot, E.; Maréchal, J.-P.; Fayad, V.; David, G.; Sidi Cheikh, M.; Failler, P. Mapping Coastal Marine Ecosystems of the National Park of Banc d'Arguin (PNBA) in Mauritania Using Sentinel-2 Imagery. *Int. J. Appl. Earth Obs. Geoinf.* **2021**, *102*, 102419. [CrossRef]
78. Roelfsema, C.; Kovacs, E.; Ortiz, J.-C.; Callaghan, D.; Hock, K.; Mongin, M.; Johansen, K.; Mumby, P.; Wettle, M.; Ronan, M.; et al. Habitat Maps to Enhance Monitoring and Management of the Great Barrier Reef. *Coral Reefs* **2020**, *39*, 1039–1054. [CrossRef]
79. Van An, N.; Quang, N.H.; Son, T.P.H.; An, T.T. High-Resolution Benthic Habitat Mapping from Machine Learning on PlanetScope Imagery and ICESat-2 Data. *Geocarto Int.* **2023**, *38*, 2184875. [CrossRef]
80. Hochberg, E.J.; Atkinson, M.J.; Andréfouët, S. Spectral Reflectance of Coral Reef Bottom-Types Worldwide and Implications for Coral Reef Remote Sensing. *Remote Sens. Environ.* **2003**, *2*, 159–173. [CrossRef]
81. Wicaksono, P.; Lazuardi, W. Assessment of PlanetScope Images for Benthic Habitat and Seagrass Species Mapping in a Complex Optically Shallow Water Environment. *Int. J. Remote Sens.* **2018**, *39*, 5739–5765. [CrossRef]
82. Nasrul, M.R.; Wicaksono, P.; Arjasakusuma, S. Live and Dead Coral Cover Mapping Using PlanetScope Image around Mandangin Island, Madura, Indonesia. In Proceedings of the Seventh Geoinformation Science Symposium 2021, Yogyakarta, Indonesia, 25–28 October 2021; Volume 12082, pp. 141–149.
83. Kovacs, E.; Roelfsema, C.; Lyons, M.; Zhao, S.; Phinn, S. Seagrass Habitat Mapping: How Do Landsat 8 OLI, Sentinel-2, ZY-3A, and Worldview-3 Perform? *Remote Sens. Lett.* **2018**, *9*, 686–695. [CrossRef]
84. Zhang, C. Applying Data Fusion Techniques for Benthic Habitat Mapping and Monitoring in a Coral Reef Ecosystem. *ISPRS J. Photogramm. Remote Sens.* **2015**, *104*, 213–223. [CrossRef]

Disclaimer/Publisher's Note: The statements, opinions and data contained in all publications are solely those of the individual author(s) and contributor(s) and not of MDPI and/or the editor(s). MDPI and/or the editor(s) disclaim responsibility for any injury to people or property resulting from any ideas, methods, instructions or products referred to in the content.